SFF-Oriented Modeling and Process Planning of Functionally Graded Materials using a Novel Equal Distance Offset Approach

Anping Xu[1] and Leon L. Shaw[2]

[1] School of Mechanical Engineering, Hebei University of Technology
Tianjin 300130, P. R. China
Email: mcad@hebut.edu.cn
[2] Department of Metallurgy and Materials Engineering, Institute of Materials Science
University of Connecticut, Storrs, CT 06269, USA

Abstract

This paper deals with the modeling and process planning of solid freeform fabrication (SFF) of 3D functionally graded materials (FGMs). A novel approach of representation and process planning of FGMs, termed as equal distance offset (EDO), is developed. In EDO, a neutral arbitrary 3D CAD model is adaptively sliced into a series of 2D layers. Within each layer, 2D material gradients are designed and represented via dividing the 2D shape into several sub-regions enclosed by iso-composition contours. If needed, the material composition gradient within each of sub-regions can be further determined by applying the equal distance offset algorithm to each sub-region. Using this approach, an arbitrary-shaped 3D FGM object with linear or non-linear composition gradients can be represented and fabricated via suitable SFF machines.

Keywords: Equal distance offset; Functionally graded materials; Solid freeform fabrication; Modeling; Process planning; Arbitrary-shaped objects

1. Introduction

Solid Freeform Fabrication (SFF) has a great potential to fabricate heterogeneous objects. In recent years SFF has been increasingly used in biomaterial related applications such as dental restorations, orthopedic implants, scaffolds, and drug delivery where complex-shaped objects made of multiple materials or functionally graded materials are typically desired. To model a functionally graded material (FGM) object, a CAD system should first be able to know the material composition of each point of the object. But unfortunately, the traditional geometrical solid modeling has focused on modeling the geometry and topology of the object. The most commonly used representation schemes for the traditional models are the Constructive Solid Geometry (CSG), Boundary Representation (B-Rep), or a hybrid of these schemes [1]. All these representation methods are not capable of including the material composition information.

Recently, several FGM modeling and representation methods have been reported [1-11]. These methods have allowed designers to design not only the geometry, but also the material distribution of an object. However, all of these methods have mainly focused on simple-shaped FGM objects with simple gradient schemes. It is very difficult (or impossible

in some cases) to use these methods to process arbitrary-shaped FGM objects with authentic 3D gradients. Kumar and Dutta [1-3] have presented an approach using regular sets (*r-sets)* extended to include composition r_m-*sets* with accompanying Boolean operators. An r_m-object is defined as a finite collection of the r_m-*sets* with each r_m-*set* being a material domain with an analytical material function. Jackson, et al. [10] have introduced an approach that is based on subdividing the solid model into sub-regions (tetrahedrons) and associating an analytic composition blending function with each region to define the material composition. Pegna and Sali [11] have proposed a model by representing multi-material models as point set including Cartesian coordinates plus the material composition. Although these approaches can theoretically model the FGM object with complex gradients, it suffers from the disadvantages of requiring an enormous amount of storage space.

Unlike the other heterogeneous object representation schemes, Siu and Tan [7,8] and Zhou, et al. [9] have presented modeling methods in which the discretization of the material composition is done in 2D layer rather than in 3D space. Furthermore, the material composition is expressed in terms of distance functions with a single entity or multiple entities as the reference(s). Compared to finite cell, *r-sets,* or point set approaches [1-3,10,11], storing material information in terms of distance functions has greatly saved much memory. In spite of this advantage, the method proposed by Siu and Tan can only be used for FGMs with simple geometry and composition gradients because the reference for the distance function is a simple geometrical shape such as a point, a plane, or a line [7,8]. Similarly, the method by Zhou, et al. is also limited to FGMs with relatively simple geometry and composition gradients, because different compositions may be obtained at the same point or the composition may not be the desired one when the multiple references must be used for complex-shaped objects [9]. Thus, it is necessary to develop new representation and processing methods for modeling FGMs in order to meet the requirement of modeling and fabrication of 3D complex-shaped FGM objects.

In this paper, a novel approach of representation and process planning of FGMs, termed as equal distance offset (EDO), is developed. In EDO, a neutral arbitrary 3D CAD model is adaptively sliced into a series of 2D layers. Within each layer, 2D material gradients are designed and represented via dividing the 2D shape into several sub-regions enclosed by iso-composition boundaries, which is then followed by applying the equal distance offset algorithm to each sub-region. Using this approach, an arbitrary-shaped 3D FGM object with linear or non-linear composition gradients can be represented and fabricated via suitable SFF machines. This EDO approach is described in the following several sections.

2. Reconstruction of Neutral Complex-Shaped 3D Objects

In most cases, practical complex-shaped 3D modeling will start with medical computed tomography (CT) images, any commercial CAD modelers (such as EDS UGS NX, Pro/E, etc.), or point clouds obtained from a coordinate measuring machine (CMM). For medical applications, the medical CT images that are obtained from patient specific implants can provide detailed information about the regional structure and function of the patient implants. Alternatively, for general purposes, it can start with any commercial CAD modelers or point clouds from CMM. A different modeling approach can be selected for different data sources.

For the medical CT images, commercial software, such as 3D-Doctor (Able Software Corp. Lexington, MA, USA) or Mimics (Materialise, Belgium), can be used to reconstruct the 3D CAD model. In order to accomplish the 3D CAD reconstruction, the 3D model needs to be sliced into a series of 2D layers first. These slices should then be segmented to separate the various tissues according to the optimized gray tone threshold. After this, the connected components analysis needs to be done so that the topological relationship between different tissues can be successfully established. Once all slices have been processed, 3D volumetric models can be easily generated based on the Computer-Aided Geometrical Design (CAGD) theory and data fitting methods. It is noted that there is no material information included in this stage. For the point clouds data source, a 3D model can also be built using some commercial software such as Magics RP (Materialise, Belgium). Similarly, there is no material information included in this stage of the 3D CAD model. Thus, the next step is to integrate the material information into the CAD model.

3. The EDO Approach to Designing and Representing 3D Graded Objects

In order to integrate the material information into the neutral freeform CAD model, the 3D CAD model should be translated into IGES format, which is then discretized into a series of slices along the building direction (set it in the Z-direction) using adaptive slicing method [12], and the layer thickness here will be determined by the Z-directional local slope and the desired gradient step-width in the Z-direction. Then, for each thin slice, only 2D gradients need to be designed and represented. Figure 1 shows one of the most complicated situations, in which the thin slice consists of one internal boundary C_i and one external boundary C_e, and the material composition should be continuously changed from the internal boundary C_i to the external boundary C_e.

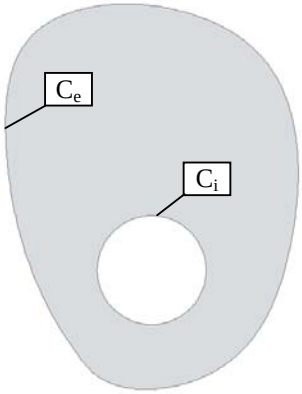

Figure 1. 2D sliced complex-shaped region without material information.

3.1 Pre-Subdivision of 2D Regions

In order to represent the 2D region with material composition gradients, subdivision should be done first. To do this, a cluster of radial lines from the geometrical center of the internal boundary C_i should be generated with an equal angular division within 360^0. As shown in Figure 2(a), each radial line between internal and external boundaries is uniformly divided into m segments (m = 10 in the example shown). m can be determined by the fabrication capability of the spatial resolution of the SFF machine and the design requirement for material gradients. For example, m can be set to equal the length of the shortest radial line on the 2D slice, L_{short} [see Fig. 2(a)], divided by the spatial resolution of the SFF machine selected, R_{mach}:

$$m = \text{int}\left(\frac{L_{short}}{R_{mach}} + 0.5\right) \tag{1}$$

Thus, the length of the smallest segment in any radial line on the 2D slice will be R_{mach}. Further, any local sub-area enclosed by the segments with a length smaller than R_{mach} cannot

be fabricated by the SFF machine selected. Once *m* is determined, a series of spline curves, like growth rings, are then generated passing through the corresponding division points [Fig. 2(b)]. Figure 2(c) is the final 2D sub-regions enclosed by spline curves after subdivision.

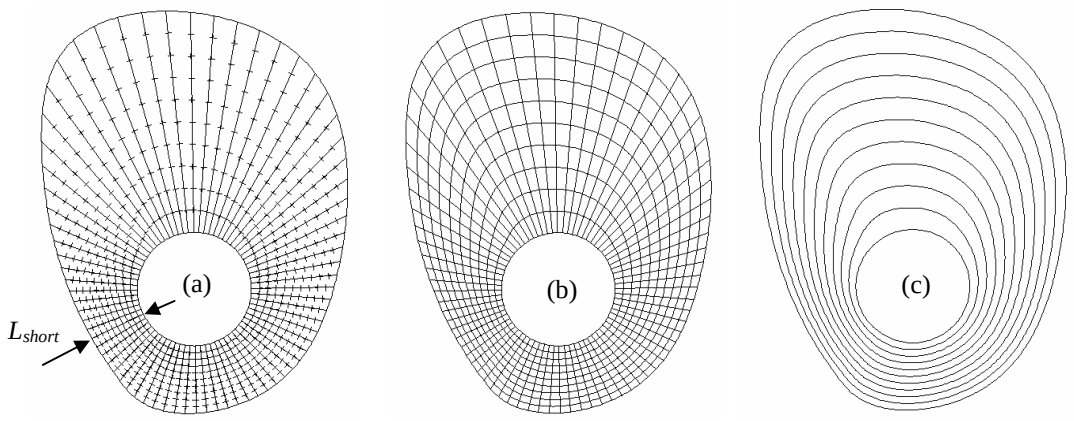

Figure 2. Description of the algorithm for 2D regional subdivision: (a) radial lines with an equal angular division, (b) a series of spline curves passing through the corresponding division points, and (c) the final 2D sub-regions enclosed by spline curves after subdivision.

3.2 EDO Approach to Representation of Sub-Regional FGMs

In order to incorporate the material information into the sub-regions, the next step is to determine a gradient direction, such as the arrow direction ***g*** shown in Fig. 3(a), which coincides with any one of the previous radial lines and the origin point starts at the intersection point with the internal boundary C_i. The following step is then to define a material array ***M*** for mapping the material information for every spline curve (called as contour hereafter) surrounding the sub-region. Each element of the material array ***M*** represents the volume fraction of one of the pre-defined primary materials. For every contour, it should be subject to the relationship $\sum_{j=1}^{n} M_j = 1$, where M_j denotes the j^{th} element of the material array ***M*** and *n* is the number of the pre-defined primary materials.

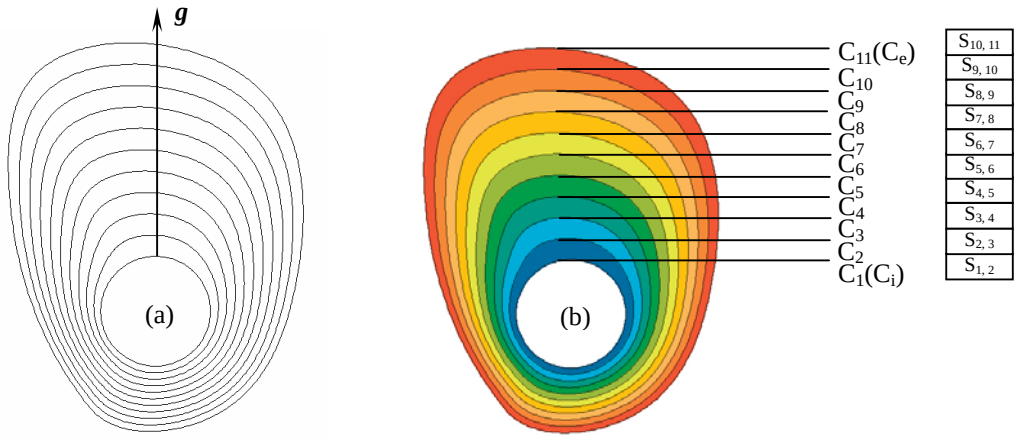

Figure 3. EDO approach to representation of sub-regional FGMs: (a) determination of gradient direction and (b) relationship between contours and sub-regions.

Suppose that the distance from the internal boundary to the external boundary in $\boldsymbol{g}$ direction is 1, and (m – 1) contours are generated from the internal to the external boundary. As shown in Figure 3, C_2, C_3, … and C_{10} represent the contours to divide the 2D sliced region, and $S_{1,2}$, $S_{2,3}$, … and $S_{10,11}$ represent the sub-regions surrounded by C_1 and C_2, C_2 and C_3, … and C_{10} and C_{11}, respectively. In this case, the distance from the internal boundary C_i (i.e., C_1) to the j^{th} (j = 1, 2, …, m+1) contour (or boundary) can be expressed as

$$d_j = \frac{j-1}{m} \qquad (j = 1, 2, \ldots, m+1) \tag{2}$$

Thus the gradient material distribution function can be defined either linearly or nonlinearly as $f(d_j)$, where

$$f(d_j) = \begin{cases} 0 & \text{for } d_j = 0 \\ f(d_j) \in (0,1) & \text{for } d_j \in (0,1), \text{but to be discrete} \\ 1 & \text{for } d_j = 1 \end{cases} \tag{3}$$

For example, if linear, it can be expressed as $f(d_j) = Ad_j + B$, where A and B are constants. When A = 1 and B = 0, the gradient material distribution function can then be reduced to $f(d_j) = d_j$. Suppose that the material composition arrays corresponding to C_i and C_e are $\boldsymbol{M}(C_i)$ and $\boldsymbol{M}(C_e)$, respectively, and the material composition arrays between C_i and C_e vary continuously from one end to another, then the material composition array corresponding to the j^{th} contour can be expressed as

$$\boldsymbol{M}(C_j) = f(d_j) \cdot \left(\boldsymbol{M}(C_e) - \boldsymbol{M}(C_i)\right) + \boldsymbol{M}(C_i) \tag{4}$$

Further assume that there are two kinds of materials named as MA and MB involved in the FGM, and from contours C_i to C_e, the material composition changes continuously from [1, 0] to [0, 1]. As shown in Figure 3, the material composition arrays for C_4 and C_5 can be obtained using Eq. (4) as follows.

$$\boldsymbol{M}(C_4) = \frac{4-1}{10} \cdot \left([0 \quad 1] - [1 \quad 0]\right) + [1 \quad 0] = [0.7 \quad 0.3]$$

$$\boldsymbol{M}(C_5) = \frac{5-1}{10} \cdot \left([0 \quad 1] - [1 \quad 0]\right) + [1 \quad 0] = [0.6 \quad 0.4]$$

In each sub-region, further sub-division may be required in order to represent the composition change in the local area. This can be done by repeatedly using the EDO method to each sub-region such as $S_{2,3}$, $S_{3,4}$, … and $S_{9,10}$ shown in Figure 3(b). However, for sub-regions $S_{1,2}$ and $S_{10,11}$, due to the consideration of material continuity and homogeneity on the surface, the boundaries C_1 and C_{11} must be geometrically offset outwards and inwards, respectively. The offset distance value depends on the fabrication capability of the spatial resolution of the SFF machine. For example, if the FGM object is to be fabricated using an extrusion machine, the offset distance will then be equal to or proportional to the diameter of the extrusion nozzle.

The spatial resolution of the material composition in each sub-region is also limited by the fabrication resolution of the SFF machine, and the material composition gradient within each sub-region can be obtained by applying the interpolation algorithm of equal distance offset between two adjacent contours, subjecting to the limitation of the fabrication resolution of the SFF machine. Suppose that (i) an extrusion-based SFF machine is used to build the FGM, (ii) the diameter of the extrusion nozzle is D_{noz}, and (iii) the maximum distance in the gradient direction $\boldsymbol{g}$ between two adjacent contours is $D_{\max}$, then the maximum number of equal distance offsets $N_{\max}$ in sub-region $S_{n,n+1}$ can then be calculated as

$$N_{\max} = \text{int}\left(\frac{D_{\max}}{D_{\text{noz}}} + 0.5 \right) \tag{5}$$

and the material composition array for the i-th (counting from the offset contour but not including itself) equal distance offset in sub-region $S_{n,n+1}$ can be expressed as

$$\boldsymbol{M}\left(S_{n,n+1}, i\right) = \begin{cases} \dfrac{i}{N_{\max}} \cdot \left(\boldsymbol{M}(\mathrm{C}_n) - \boldsymbol{M}(\mathrm{C}_{n+1})\right) + \boldsymbol{M}(\mathrm{C}_{n+1}) & \text{for offsetting inwards} \\ \dfrac{N_{\max} - i}{N_{\max}} \cdot \left(\boldsymbol{M}(\mathrm{C}_n) - \boldsymbol{M}(\mathrm{C}_{n+1})\right) + \boldsymbol{M}(\mathrm{C}_{n+1}) & \text{for offsetting outwards} \end{cases}$$

$$(i = 1, 2, \cdots, N_{\max} - 1) \tag{6}$$

The step width array of the composition change in sub-region $\mathrm{S}_{n,n+1}$ can be calculated as

$$\boldsymbol{W}\left(S_{n,n+1}\right) = \boldsymbol{M}\left(S_{n,n+1}, i+1\right) - \boldsymbol{M}\left(S_{n,n+1}, i\right) \tag{7}$$

$\boldsymbol{W}(S_{n,n+1})$ is a constant vector in the same 2D sub-region since a linear interpolation algorithm [Eq. (6)] is applied between two adjacent contours. However, in general $\boldsymbol{W}(S_{n,n+1})$ can be a variable if the composition gradient within the sub-region is not linear and a non-linear interpolation algorithm is applied. Nevertheless, there are advantages in using a linear composition gradient within a sub-region. For a linear composition gradient, only one step width array needs to be memorized in the computer for each sub-region. In addition to this step width array, the other information needed for fabrication of each sub-region is the material composition array corresponding to either of two adjacent contours and the number of equal distance offsets. Thus, computer memory can be greatly saved if a linear composition gradient within each sub-region is adopted.

Again sub-region $\mathrm{S}_{4,5}$ enclosed by contours C_4 and C_5 can be used to illustrate the application of Eqs. (6) and (7). As mentioned above, the corresponding materials composition arrays for contours C_4 and C_5 are $\boldsymbol{M}(\mathrm{C}_4)$ = [0.7 0.3] and $\boldsymbol{M}(\mathrm{C}_5)$ = [0.6 0.4], respectively. Assuming $N_{\max}$ = 4 as shown in Fig. 4(a), the material composition array for each of the equal distance offsets can be calculated using Eq. (6) as follows.

$$\boldsymbol{M}\left(\mathrm{S}_{4,5}, 1\right) = \frac{1}{4} \cdot \left([0.7 \quad 0.3] - [0.6 \quad 0.4]\right) + [0.6 \quad 0.4] = [0.625 \quad 0.375]$$

$$\boldsymbol{M}\left(\mathrm{S}_{4,5}, 2\right) = \frac{2}{4} \cdot \left([0.7 \quad 0.3] - [0.6 \quad 0.4]\right) + [0.6 \quad 0.4] = [0.65 \quad 0.35]$$

$$\boldsymbol{M}\left(\mathrm{S}_{4,5}, 3\right) = \frac{3}{4} \cdot \left([0.7 \quad 0.3] - [0.6 \quad 0.4]\right) + [0.6 \quad 0.4] = [0.675 \quad 0.325]$$

Note that the i^{th} equal distance offset above is counted starting from contour C_5. Also, using Eq. (7), the step width array of the composition change in sub-region $S_{4,5}$ can be obtained as

$$\boldsymbol{W}(S_{4,5}) = [0.025 \quad -0.025]$$

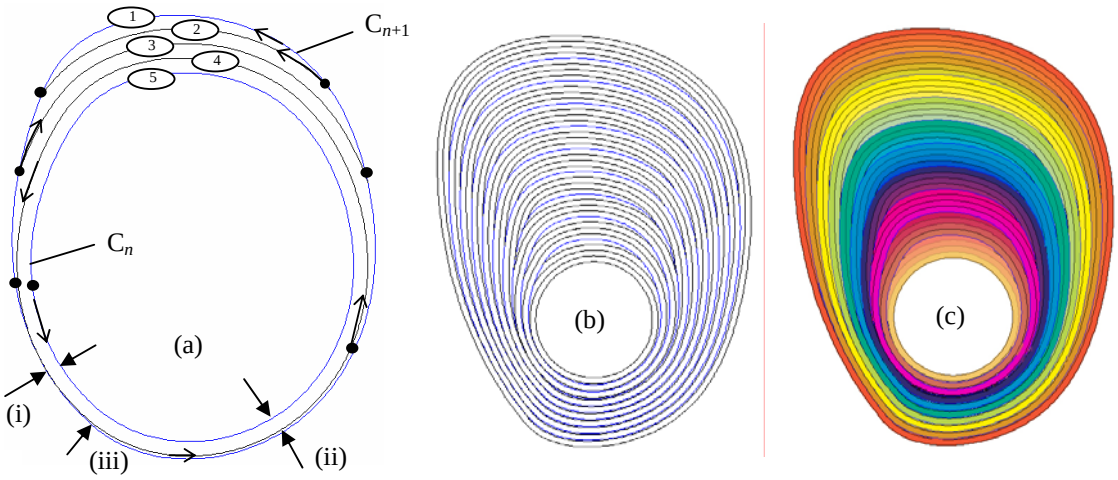

Figure 4. Process planning of functionally graded objects: (a) filling paths planning of sub-region $S_{n,n+1}$, (b) the entire filled region, and (c) the filled region with the rendering effect. The paths 1 to 5 in (a) represent the filling sequence and ● stands for the starting and/or ending point for the filling paths.

4. Process Planning Method of Functionally Graded Objects

After incorporating the material information into every 2D layer, the next step will be process planning of functionally graded objects. Assuming that the FGM object is to be fabricated using an extrusion machine [13], then to build the EDO-based functionally graded material, the extrusion nozzle has to move along the iso-composition contours and equal distance offsets according to the specified scanning paths, which are a combination of non-continuous segments and closed loops. Figure 4(a) shows the scanning path of the extrusion nozzle, where C_n and C_{n+1} stand for two adjacent iso-composition contours with two different material composition arrays; the arrows stand for the scanning directions; and the sequence in filling the sub-region along the 2 iso-composition contours (closed loops) and 3 equal distance offsets (non-continuous segments) is marked by the numbers. Note that the material composition needs to be changed from one filling path to another by the step width array $\boldsymbol{W}$, i.e., the composition changes from path 1 to path 2, then from path 2 to path 3, and so on. However, on each of the iso-composition contours and equal distance offsets, the material composition stays the same. Also note that the filling is not continuous, i.e., at the ending point a temporary cessation of extrusion will be applied, while the nozzle moves from the ending point to a new starting point. Figure 4(b) demonstrates the entire filled region, and Figure 4(c) shows the filled region with the rendering effect.

The selection of the starting and ending points during extrusion is closely related to the fabrication capability of the spatial resolution of the SFF machine. In some narrow sub-areas or at some intersections between contours and equal distance offsets, flaws (e.g.,

porosity) or staircase effect could occur in the process of fabrication. Such flaws and staircase effect can, however, be minimized or eliminated if the starting and ending points as well as the extrusion rate (i.e., the volume of the slurry extruded per unit time through the extrusion nozzle) have been judicially selected or adjusted. One important example in eliminating the flaw in a narrow sub-area is presented in Fig. 4(a). At the location marked as (i) only two extrusion paths (C_n and C_{n+1}) are allowed due to the spatial resolution of the nozzle diameter. However, at the location marked as (ii) it would require more than two extrusion paths, but less than three extrusion paths (e.g., need 2.3 paths) to fill the space. To solve this problem, the extrusion rate would be increased starting from the location (iii), while maintaining a constant scanning rate. Thus, the width of the extrudate will increase to 1.3 for extrusion path C_n (or C_{n+1}). As a result, there will be no flaw (e.g., pores) at the region around the location (ii). During implementation of the EDO-based integrated program, another factor should also be included in the program, that is, the nozzle radius compensation needs to be considered like tool radius compensation during conventional NC machining. This issue will be addressed in the future study.

5. Conclusions

A novel approach of representation and process planning of FGMs, termed as equal distance offset (EDO), is developed in this paper. The proposed approach can be applied to arbitrary-shaped objects with 3D material composition gradients. Three different kinds of 2D gradient distribution patterns most probably encountered in bioengineering are shown in Figure 5. The representation of these distribution patterns can be simply obtained by applying equal distance offset algorithm to the iso-composition contours, and no sub-region division is required in these cases. The representation of these distribution patterns will be Bezier or NURBS curves (or segmented Bezier or NURBS curves) in either open or closed form. During implementation of the EDO-based integrated program, there could be flaws or staircases in some narrow sub-areas or at some intersections between contours and equal distance offsets. Such flaws are inevitable in some cases due to the limitation of the spatial resolution of the SFF machine. However, the adverse effect of such flaws can be minimized or eliminated through judicial selection of the starting and ending points for each filling (or scanning) path and the adjustment of the extrusion rate during extrusion if an extrusion-based SFF machine is used.

Future studies on the EDO approach will focus on (a) the minimization of staircases and flaws at the intersection of the iso-composition contours and the equal distance offsets and at the narrow sub-areas where fabrication of the sub-area demands non-integral fabrication paths to eliminate porosity, (b) the implementation of the EDO integrated program based on the application programming interface (API) of EDS UGS NX, and (c) the inclusion of the nozzle radius compensation, the support structure design and part orientation issues in the program.

Acknowledgements – The first author AX would like to thank the Service Center for Experts and Scholars of Hebei Province, China for providing the financial support (No.2001-21), while LS gratefully acknowledges the financial support provided by the U.S. National

Science Foundation under Grant Nos: DMI-9908249 and DMI-0218169.

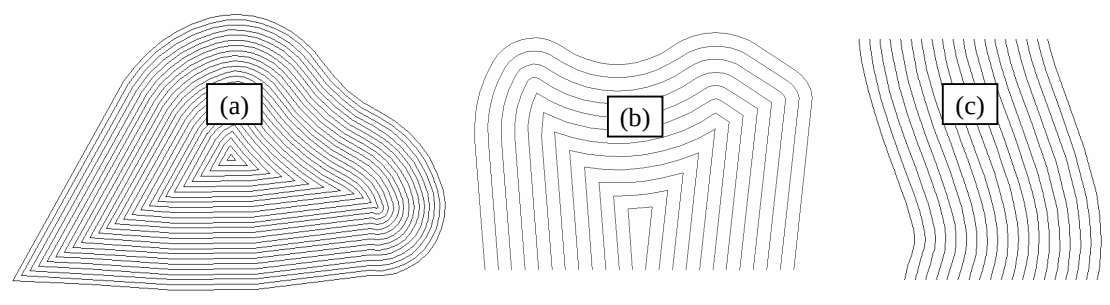

Figure 5. Three different kinds of 2D gradient distribution patterns in bioengineering: (a) growth- ring-like contours, (b) tooth-crown-like contours, and (c) fiber-like contours.

References

1. D. Dutta and V. Kumar, "Process planning for layered manufacturing using heterogeneous solid models," in Proc. of the 3rd Pacific Rim International Conference on Advanced Materials and Processing (PRICM 3), M.A. Imam, et al. (Eds.), 1998.
2. V. Kumar and D. Dutta, "An approach to modeling multi-material objects," in Proc. of Solid Modeling '97, Altanta, GA, 336-345, 1997.
3. V. Kumar and D. Dutta, "An approach to modeling and representation of heterogeneous objects," J. Mech. Des., 120 (12): 659-667, 1998.
4. S. Bhashyam, K. H. Shin, and D. Dutta, "An Integrated CAD System for Design of Heterogeneous Objects," Rapid Prototyping Journal, Vol.6 (2): 119-135, 2000.
5. K. H. Shin, H. Natu, D. Dutta, and J. Mazumder, "A method for the design and fabrication of heterogeneous objects," Materials & Design, 24 (2003): 339-353.
6. L. Patil, D. Dutta, A. D. Bhatt, K. Jurrens, K. Lyons, M. J. Pratt, R. D. Sriram, "Representation of Hetergeneous Objects in ISO 10303 (STEP)," in Proc. of the ASME Conference, Orlando, FL, November 2000.
7. Y. K. Siu and S. T. Tan, "Slicing and contours generation for fabricating heterogeneous objects," in Proceedings of the Geometric Modeling and Processing – Theory and Application, 2002.
8. Y. K. Siu and S. T. Tan, "Source-based hetergeneous solid modeling," Comput. Aided Des., 34: 41-55 (2002).
9. M. Y. Zhou, J. T. Xi, and J. Q. Yan, "Modeling and processing of functionally graded materials for rapid prototyping," Journal of Materials Processing Technology, 146 (2004): 396–402.
10. T. R. Jackson, H. Liu, N. M. Patrikalakis, E. M. Sachs, and M. J. Cima, "Modeling and designing functionally graded material components for fabrication with local composition control," Materials & Design, 20 (1999): 63-75.
11. J. Pegna and A. Sali, "CAD modeling of multi-model structures for freeform fabrication," in Proc. of the 9th Solid Freeform Fabrication Symposium, Austin, TX, August 1998.
12. Y. Liu and A. Xu, "An effective direct slicing algorithm of CAD model and its implementation," Journal of Hebei University of Technology, 2003, 32(5): 35-38.
13. L. Shaw, "A Novel SMD Machine for Solid Freeform Fabrication of FGMs," University of Connecticut Invention Disclosure, July 2004.